First-principles calculations of phonon dispersion and lattice dynamics in La_2CuO_4

Cheng-Zhang Wang, Rici Yu, and Henry Krakauer
Department of Physics, College of William and Mary, Williamsburg, Virginia 23187-8795
(Received 24 September 1998)

First-principles density-functional linearized augmented plane-wave linear-response calculations are presented of the lattice dynamics of tetragonal La_2CuO_4. Phonon frequencies and eigenvectors are obtained throughout the Brillouin zone. Generally good agreement is achieved with experiment, but frequencies of the lowest-lying branches, which involve anharmonic motion of the apical oxygen atoms parallel to the CuO_2 planes, are underestimated. The octahedral tilt mode at the X point is found to be the most unstable mode throughout the Brillouin zone, consistent with the observed phase transition to the orthorhombic structure at low temperature. The calculated dispersion of the highest frequency Σ_3 branch is in good agreement with experiment, showing that a proposed large renormalization of the phonon spectrum by a Jahn-Teller electron-phonon interaction is unlikely. [S0163-1829(99)12513-X]

I. INTRODUCTION

Studies of lattice-dynamical properties in high-temperature superconductors (HTS) have been a focus of interest ever since their discovery. There are many experimental observations of strong electron-phonon interactions,[1–3] and while considerable doubt has been expressed regarding the adequacy of solely a conventional electron-phonon mechanism to account for high-T_c superconductivity,[4] this mechanism is clearly present and may play an important role. It is thus important to fully characterize the lattice-dynamical properties of the HTS. Due to its simple crystal structure, the single layer compound $La_{2-x}Sr_xCuO_4$ has been the subject of many experimental and theoretical investigations. The analysis of its phonon properties is complicated, however, by a structural phase transition from the high-temperature tetragonal phase to the low-temperature orthorhombic phase, which is driven by the softening of the tilt mode at the Brillouin-zone boundary X point.[5] Moreover, as in many other HTS compounds, phonon frequencies of $La_{2-x}Sr_xCuO_4$ have been studied with different experimental probes, but much less is known about the corresponding eigenvectors. This makes the mode assignments sometimes difficult.

First-principles local density-functional approximation (LDA) calculations correctly predicted the tilt mode instability and the relevant atomic displacements in the phase transition.[6] This success indicates that the many-body interactions beyond LDA have little effect on the structural phase transition. Subsequent first-principles calculations obtained the full Γ phonon spectra and a few X-point phonons in La_2CuO_4,[6–8] as well as the high-symmetry Γ phonons in $YBaCu_3O_7$,[9–11] which are in good agreement with experiment. This suggests that LDA calculations can accurately predict the static density response and that phonons are not heavily dressed by spin or excitonic fluctuations in the HTS. In this paper first-principles LDA linear response calculations are presented of the phonon dispersions and eigenvectors of tetragonal La_2CuO_4 throughout the Brillouin zone.

II. METHOD

The calculations are carried out using the LAPW (linearized augmented plane-wave) linear response method,[12] implemented with the Steinheimer approach.[13] The use of LAPW basis functions facilitates the treatment of localized valence wave functions such as those derived from Cu($3d$) and O($2p$) orbitals. Unlike the supercell ''frozen phonon'' approach, the linear response (or density-functional perturbation) method can determine the electronic response to perturbations such as periodic lattice distortions of arbitrary wavelength, while keeping the numerical complexity of the calculation similar to a self-consistent calculation for the unperturbed system. On the other hand, the use of finite differences in the frozen phonon approach yields information about anharmonic effects, which are inaccessible within linear response. The dynamical matrix elements for a given wave vector $\mathbf{q}$ are found via the first-order forces, calculated for at most $3N$ selected atomic displacements at each wave vector, where N is the number of atoms in the primitive cell. Phonon vibrational frequencies and polarization vectors are obtained by diagonalizing the dynamical matrix $D(\mathbf{q})$. To map the phonon-dispersion curves throughout the Brillouin zone, the dynamical matrix is obtained on a uniform $4\times4\times2$ grid of q points, and real-space force constants are then found by Fourier transform of the dynamical matrix. The dynamical matrix at an arbitrary wave vector $\mathbf{q}$ can then be computed by an inverse Fourier transform.

Kerker pseudopotentials[14] were used to bypass the need to treat the chemically inert localized inner core states. The atomic states La ($5s$,$5p$,$5d$,$4f$), Cu ($4s$,$4p$,$3d$), and O ($2s$,$2p$) were pseudized and treated variationally in the computation. The Wigner interpolation formula[15] was used for the exchange-correlation potential. Brillouin-zone integrations used a uniform $8\times8\times2$ k-point mesh,[16] yielding 128 k points in the full Brillouin zone of the body-centered tetragonal structure, and temperature broadening[17] was employed to accelerate convergence. Test calculations indicated that this k-point mesh yields phonon frequencies that are converged to within about 1%. This is consistent with Singh's (Ref. 8) convergence tests. He used a

TABLE I. Calculated phonon frequencies and eigenvectors of the dynamical matrix. Note that the atomic displacements may be obtained by dividing the eigenvector components by the square root of the atomic mass. Atoms in A_{1g}, A_{2u}, and B_{2u} modes move along the $\hat{c}$ direction, while atoms in E_{1g} and E_u modes move along the **x** direction. The atom labels are explained in the text.

Mode	Frequency (cm^{-1})	Eigenmode						
		La(1)	La(2)	Cu	O(1)	O(2)	O(3)	O(4)
A_{1g}	202	−0.70	0.70	0	0	0	0.07	−0.07
A_{1g}	375	0.07	−0.07	0	0	0	0.70	−0.70
A_{2u}	132	−0.33	−0.33	0.87	0.12	0.12	−0.02	−0.02
A_{2u}	182	−0.21	−0.21	−0.28	0.50	0.50	0.41	0.41
A_{2u}	441	0.07	0.07	−0.10	0.45	0.45	−0.54	−0.54
B_{2u}	193	0	0	0	−0.71	0.71	0	0
E_{1g}	26	−0.66	0.66	0	0	0	−0.26	0.26
E_{1g}	201	0.26	−0.26	0	0	0	−0.66	0.66
E_u	22	0.25	0.25	−0.07	−0.06	0.05	−0.66	−0.66
E_u	147	0.31	0.31	−0.71	−0.32	−0.38	0.16	0.16
E_u	319	−0.01	−0.01	−0.43	−0.08	0.90	0.06	0.06
E_u	630	0	0	−0.38	0.92	−0.10	−0.03	−0.03

$6\times6\times2$ k-point mesh and found only 3% changes in the frequency upon increasing to an $8\times8\times2$ mesh. The latter denser mesh is the mesh size we used in the present studies. In the linear response computations, de Girocoli's smearing technique,[18] was used to deal with the fractional occupation around the Fermi level. We used approximately 750 LAPW basis functions, which converges the phonon frequencies to within an error of about 2%.

The calculations were performed with respect to the ideal tetragonal structure with lattice parameters $a=3.79$ Å and $c=13.21$ Å.[19] The atomic positions are given by La(1), $(0,0,0.362c)$; La(2), $(0,0,-0.362c)$; Cu, (0, 0, 0); O(1), $(0.5a,0,0)$; O(2), $(0,0.5a,0)$; O(3), $(0,0,0.182c)$; and O(4), $(0,0,-0.182c)$, where the O(1) and O(2) atoms are in the CuO_2 planes, and the O(3) and O(4) are the apical oxygens.

III. RESULTS AND DISCUSSION

A. Phonons at Γ

The full phonon spectra consists of 21 phonon modes, three acoustic, and 18 optic modes. Table I presents vibrational frequencies and eigenvectors of optic-phonon modes at the Γ point. Note that the eigenvectors are the actual displacements weighted by the square root of atomic mass. According to their symmetry, these 18 optic phonons are represented as $2A_{1g}+3A_{2u}+B_{2u}+2E_g+4E_u$. The atomic displacements in A_{1g}, A_{2u}, and B_{2u} modes are all along the $\hat{c}$ direction. The E_g and E_u modes are doubly degenerate and the atomic displacements are parallel to CuO_2 planes. Table II compares the phonon frequencies with experiment and two LDA frozen phonon calculations. The good agreement with Singh's frozen phonon results[8] provides a useful cross-check of the two methods.

The two A_{1g} have inversion symmetry and are thus Raman active and involve only the displacements of La and apical O atoms along the $\hat{c}$ direction. While both modes change the bond lengths of La(1)-O(3) and Cu-O(3), they differ significantly in frequency, because La is much heavier than O, with the mode involving primarily La displacement having a lower frequency than the mode which is dominated by O displacements. Our phonon frequencies of A_{1g} modes are in good agreement with previous LDA calculations and measurements from neutron and Raman-scattering experiments.

There are three A_{2u} modes, which have no inversion symmetry and hence are infrared (IR) active. The calculated frequencies of these three modes are 132, 182, and 441 cm^{-1}.

TABLE II. Zone-center phonon frequencies (in cm^{-1}).

Mode	Present	LDA [a]	LDA [b]	IR	Neutron [e]	Raman [f]
A_{1g}	202	215	224		227	226
A_{1g}	375	390	415		427	433
A_{2u}	132	119		135[c], 242[d]	149	
A_{2u}	182	197		235[c], 342[d]	251	
A_{2u}	441	446		500[c], 501[d]	497	
B_{2u}	193	201	293		270	
E_{1g}	26	15			91	
E_{1g}	201	212	233		241	
E_u	22	75i	39		126	
E_u	147	146		140[d]	173	
E_u	319	312		360[d]	354	
E_u	630	650		695[d]	684	

[a] Singh (Ref. 8).

[b] Cohen *et al.* (Ref. 6). Note that, while A_{1g} and B_{2u} frequencies are from eigenmode calculations, E_{1g} and E_u frequencies are for pure O motions. Solving the Shrödinger equation for an anharmonic oscillator of pure O motion in the E_u mode yielded the first excitation frequency of 148 cm^{-1} (Ref. 6).

[c] Henn *et al.* (Ref. 21).

[d] Collins *et al.* (Ref. 20).

[e] Extracted from data of $La_{1.9}Sr_{0.1}CuO_4$ at 295 K (Ref. 22).

[f] Burns and Dacol (Ref. 24).

The lowest frequency A_{2u} mode consists of the vibration of Cu, along with two planar O atoms, against La atoms. The intermediate A_{2u} mode involves four O atoms vibrating against La and Cu atoms. The highest A_{2u} mode involves essentially only the O atoms, with two planar O atoms oscillating against the apical O atoms. While the phonon frequencies of the LDA calculations are in good agreement, there is a lack of consensus on the assignment of these phonon eigenmodes in experiment. In an early infrared study, Collins *et al.*[20] assigned frequencies of 242, 342, and 501 cm^{-1} to these three A_{2u} modes. More recently, Henn *et al.*[21] reported far-infrared ellipsometry measurements of the infrared-active phonon modes polarized along the $\hat{c}$ direction, yielding frequencies of 135, 235, and 500 cm^{-1}, which are consistent with both our LDA calculations and neutron-scattering data.[22] They suggested that the 342 cm^{-1} mode reported by Collins *et al.*[20] arises from Brillouin-zone folding produced by the orthorhombic distortion of the crystal, instead of from the zone center of the tetragonal phase. For the lowest A_{2u} mode, which has a very weak oscillator strength, Henn *et al.*[21] proposed the polarization vector to be a motion of La against Cu and the planar O atoms, as predicted by the present calculations, but in disagreement with Singh.[8]

The single B_{2u} mode involves only the two planar O atoms moving in opposite directions along $\hat{c}$ axis, with all other atoms undisplaced. The B_{2u} mode does not induce a dipole moment, and so is infrared inactive. The calculated phonon frequency of 193 cm^{-1} is in good agreement with Singh's calculation,[8] but smaller than the measured value[22] and an earlier LDA calculation.[6] We believe a trivial arithmetic error in calculating the frequency for this mode in Ref. 6 accounts for the discrepancy.

E_{1g} and E_u modes are doubly degenerate and all atomic displacements are parallel to the CuO_2 plane. Table I shows the representative eigenmodes along the $\hat{x}$ direction. Two of the modes are found to be soft and their harmonic frequencies are close to the accuracy limit of the calculation.[25] These two modes are the lowest E_{1g} mode and the lowest E_u mode, both involving the displacements of apical O relative to La. As shown by frozen phonon calculations, these modes exhibit very anharmonic energy vs displacement curves.[6,8] (Note that Fig. 1 in Ref. 8 uses a different energy scale from that in Ref. 6.) The present linear response calculations directly calculate only the harmonic response. Approximately including the anharmonic terms and solving the Schrödinger equation for the vibrational frequencies, Cohen *et al.*[6] obtained the lowest excitation frequency to be 148 cm^{-1} for a pure apical O symmetry E_u mode, which is comparable to the observed value. One may also expect[8] strong anharmonic interactions between these two modes and the tilt mode structural distortion to the orthorhombic phase transition to stiffen these frequencies in the orthorhombic phase. Moreover, the experimental frequencies are expected to include temperature-dependent anharmonic stiffening.

B. Phonons at *X* and *Z*

The symmetry group of the zone boundary X point, $\mathbf{q}=(\pi/a,\pi/a,0)$, is D_{2h} with eight operations. The 21 phonon modes are all nondegenerate and are represented as $4A_{1g}+3B_{1g}+3B_{2g}+2B_{3g}+3B_{1u}+3B_{2u}+3B_{3u}$. Note that the symmetry assignments in Ref. 26 are incorrect for some modes at the X point. Our calculated phonon frequencies are presented in Table III and the corresponding eigenvectors are presented in Table IV.

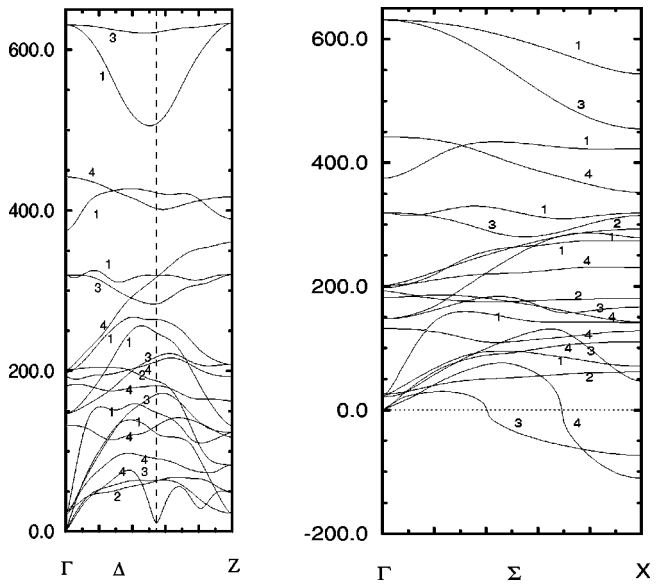

FIG. 1. Calculated phonon dispersion of tetragonal La_2CuO_4 along the $(\xi,\xi,0)$ (Σ) and $(\xi,0,0)$ (Δ) directions. The frequencies are in cm^{-1} and the imaginary frequencies are represented as negative numbers. The vertical dashed line corresponds to the boundary of the first Brillouin zone.

TABLE III. Phonon frequencies (in cm^{-1}) at the X point.

Mode	Present	LDA [a]	Expt [b]
B_{2g}	110*i*		30 (soft)
B_{2u}	73*i*		120
B_{3g}	47		137
B_{1g}	61		90
B_{1u}	71	65	150
B_{3u}	110		123*
B_{2g}	128		140
A_{1g}	141	137	150*
B_{3u}	143		153
B_{2u}	166		170
B_{1g}	180		217
B_{2g}	230		267
A_{1g}	276	263	303*
B_{1u}	278	282	310*
B_{1g}	293		317
B_{2u}	314		323
B_{1u}	319	329	373*
B_{3u}	352		407
A_{1g}	423	417	487*
B_{3g}	440		503
A_{1g}	555	642	703*

[a]Reference 7.

[b]Extracted from neutron-scattering data of Chaplot *et al.* (Ref. 23). Note that the values with symbol $*$ are from measurements of $La_{1.9}Sr_{0.1}CuO_4$ at 295 K and others are of La_2CuO_4 at 580 K.

TABLE IV. Frequencies (in cm^{-1}) and eigenvectors of phonons at the X point. For each mode, the eigenvectors are listed in the order: La(1), La(2), Cu, O(1), O(2), O(3), and O(4) as defined in the text.

	$110i$ B_{2g}			$73i$ B_{2u}			47 B_{3g}	
	Tilting			Sliding			Rotational	
−0.20	−0.20	0	0.30	−0.30	0	0	0	0
0.20	0.20	0	0.30	−0.30	0	0	0	0
0	0	0	0.03	−0.03	0	0	0	0
0	0	−0.27	0	0	0	0	0.71	0
0	0	−0.27	0	0	0	−0.71	0	0
0.42	0.42	0	−0.40	0.40	0	0	0	0
−0.42	−0.42	0	−0.40	0.40	0	0	0	0
	61 B_{1g}			71 B_{1u}			110 B_{3u}	
0.44	−0.44	0	0.45	0.45	0	0	0	−0.68
−0.44	0.44	0	0.45	0.45	0	0	0	−0.68
0	0	0	−0.08	−0.08	0	0	0	−0.26
0	0	−0.08	0	0	0	0	0	0
0	0	0.08	0	0	0	0	0	0
0.23	−0.23	0	0.22	0.22	0	0	0	−0.03
−0.23	0.23	0	0.22	0.22	0	0	0	−0.03
	128 B_{2g}			141 A_{1g}			143 B_{3u}	
0.43	0.43	0	0	0	−0.70	0	0	−0.18
−0.43	−0.43	0	0	0	0.70	0	0	−0.18
0	0	0	0	0	0	0	0	0.96
0	0	−0.32	0	0.04	0	0	0	0
0	0	−0.32	0.04	0	0	0	0	0
0.11	0.11	0	0	0	−0.04	0	0	−0.08
−0.11	−0.11	0	0	0	0.04	0	0	−0.08
	166 B_{2u}			180 B_{1g}			230 B_{2g}	
−0.39	0.39	0	−0.12	0.12	0	−0.14	−0.14	0
−0.39	0.39	0	0.12	−0.12	0	0.14	0.14	0
−0.14	0.14	0	0	0	0	0	0	0
0	0	0	0	0	−0.66	0	0	−0.57
0	0	0	0	0	0.66	0	0	−0.57
−0.30	0.30	0	0.12	−0.12	0	−0.25	−0.25	0
−0.30	0.30	0	−0.12	0.12	0	0.25	0.25	0
	276 A_{1g}			279 B_{1u}			293 B_{1g}	
0	0	−0.02	0.18	0.18	0	−0.20	0.20	0
0	0	0.02	0.18	0.18	0	0.20	−0.20	0
0	0	0	−0.31	−0.31	0	0	0	0
−0.19	0.26	0	0	0	0	0	0	0.24
0.26	−0.19	0	0	0	0	0	0	−0.24
0	0	0.63	−0.41	−0.41	0	0.43	−0.43	0
0	0	−0.63	−0.41	−0.41	0	−0.43	0.43	0
	314 B_{2u}			319 B_{1u}			352 B_{3u}	
0.09	−0.09	0	0.14	0.14	0	0	0	−0.05
0.09	−0.09	0	0.14	0.14	0	0	0	−0.05
−0.69	0.69	0	0.63	0.63	0	0	0	0.10
0	0	0	0	0	0	0	0	0
0	0	0	0	0	0	0	0	0
0.04	−0.04	0	−0.17	−0.17	0	0	0	0.70
0.04	−0.04	0	−0.17	−0.17	0	0	0	0.70
	423 A_{1g}			440 B_{3g}			555 A_{1g}	
				Quadrupolar			Breathing	
0	0	−0.05	0	0	0	0	0	−0.02
0	0	0.05	0	0	0	0	0	0.02
0	0	0	0	0	0	0	0	0
−0.10	−0.65	0	0.71	0	0	0.67	−0.03	0
−0.65	−0.10	0	0	−0.71	0	−0.03	0.67	0
0	0	0.24	0	0	0	0	0	0.21
0	0	−0.24	0	0	0	0	0	−0.21

There are two unstable modes with imaginary frequency at the X point. The first is a B_{2g} mode with frequency $110i$ cm^{-1}. This mode involves a tilt of the CuO_6 octahedra along the $(1,-1,0)$ direction, i.e., the orthorhombic x axis, with the Cu atom being fixed. The freezing in of this distortion leads to a tetragonal-orthorhombic phase transition. The instability of this mode is consistent with the neutron-scattering experiment of Böni *et al.*,[5] which shows that the tetragonal-orthorhombic phase transition is accompanied by the softening of the tilt mode at X point. At high temperature, anharmonic interactions, which are not included in the linear-response calculations, become important and stabilize the structure in the tetragonal symmetry. This tilt instability of the tetragonal structure was also found by previous LDA total energy calculations[6,7,27] and potential induced breathing (PIB) model studies.[26,28,29] The second unstable mode has B_{2u} symmetry and has a frequency of $73i$ cm^{-1}. It is labeled as a sliding mode in Table IV, involving a motion of two La atoms against the two apical O atoms, with the planar O atoms being fixed and the Cu atom essentially at rest. The sliding instability is not experimentally observed and may be stablized in the LTO phase. The absence of a phase transition corresponding to a second instability is not unusual. One well-known example is the perovskite $SrTiO_3$, which has two types of phonon instabilities in the cubic phase. There, an antiferrodistortive instability near the Brillouin-zone boundary coexists with a ferroelectric instability near the zone center. Only the antiferrodistortive phase transition to the tetragonal structure is observed, and the ferroelectric-type phase transition is never realized as the temperature is lowered.[30,31]

The frequencies and eigenvectors of the $4A_{1g}$ and $3B_{1u}$ modes have been previously reported using LDA total energy calculations.[7] Note, however, that the B_{3g} symmetry assignment in Table IV of Reference 7 is not correct, with the correct symmetry being B_{1u}. In addition, the eigenvector components reported there for the apical O and La are the sum of contributions of two equivalent atoms. The calculated phonon frequencies of the four A_{1g} modes are 141, 276, 423, and 555 cm^{-1}. The 141 cm^{-1} and 276 cm^{-1} modes consist primarily of La and apical O displacements, respectively, along the $\hat{c}$ direction. The 423 cm^{-1} mode involves planar oxygen atoms vibrating in the CuO_2 plane and perpendicular to the Cu-O bond, accompanied by axial displacements of the apical O atoms. The 555 cm^{-1} mode, labeled as the breathing mode, has the six O atoms of the CuO_6 octahedron moving together toward or away from the central Cu atom. In contrast to Weber's early parametrized calculation[32] but in agreement with previous self-consistent LDA total-energy calculations,[6,7] the breathing mode is stable and actually has the highest frequency in the full phonon spectra at X point. The calculated phonon frequencies of the three B_{1u} modes are 71, 278, and 319 cm^{-1}. All atomic displacements in these three modes are along the (1, 1, 0) direction, i.e., along the orthorhombic y axis. The 71 cm^{-1} mode involves La and apical O moving together, while the 278 cm^{-1} mode has La atoms moving oppositely to the Cu and apical O atoms. The 319 cm^{-1} mode consists of displacements of apical O atoms against the Cu and La atoms. As seen in Table III, where there is overlap, the present linear-response results for the phonon frequencies are in good agreement with those in Ref. 7. The eigenvectors of these modes are also in good agreement.

TABLE V. Phonon frequencies (in cm^{-1}) at the Z point.

Mode	This work	Neutron scattering[a]
A_{1g}	132	139
A_{1g}	390	462
A_{2u}	118	122
A_{2u}	163	180
A_{2u}	360	407
A_{2u}	417	559
B_{2u}	193	239
E_{1g}	50	123
E_{1g}	83	80
E_u	23	61
E_u	124	160
E_u	207	239
E_u	320	350
E_u	632	668

[a]Extracted from data of La_2CuO_4 at 580 K (Ref. 23).

The ''rotational'' and ''quadrupolar'' B_{3g} symmetry modes in Table IV involve only planar-O displacements within the CuO_2 planes. Contrary to the prediction of PIB model[26,28] in which only ionic interactions are considered, in the present calculations the rotational mode has a low but stable frequency of 47 cm^{-1}. Considering the light mass of the O atoms, the low frequency indicates a weak harmonic restoring force against c-axis rotations of the CuO_6 octahedra. However, total-energy calculations by Pickett *et al.* find that anharmonic restoring forces rapidly increase with increasing rotational distortion amplitude.[27] While also involving the light O atoms, the quadrupolar mode has a much higher frequency, 440 cm^{-1}, suggesting that deforming the CuO_6 octahedra is energetically unfavorable.

Like the Γ point, the zone-boundary Z point $\mathbf{q}=(0,0,\frac{\pi}{c})$ has D_{4h} symmetry, and the 21 phonons are grouped as $2A_{1g}+4A_{2u}+B_{2u}+2E_g+5E_u$. The corresponding phonon frequencies are presented in Table V together with the inelastic neutron-scattering data for comparison. The agreement with experiment is generally good except in a few cases. It should also be noted that the neutron-scattering data are collected for insulating La_2CuO_4 at high temperature 580 K, and that the calculations do not include temperature-dependent anharmonic effects. As at the Γ point, the calculations for the lowest frequency E_{1g} and E_u modes underestimate the experimental phonon frequencies, possibly for the same reasons mentioned earlier. In addition, the highest frequency A_{2u} mode is also smaller compared to experiment.

C. Phonon dispersion

Our calculated phonon dispersions along the $(\xi,\xi,0)$ (Σ) and $(\xi,0,0)$ (Δ) directions are shown in Fig. 1. For general points in the Brillouin zone, the dynamical matrices may be obtained as described in Sec. II, using a uniform $4\times4\times2$ phonon wave-vector mesh. But along the Σ and Δ directions, the dynamical matrix is calculated instead at additional

points, which correspond to an $8\times8\times2$ mesh. One-dimensional interplanar force constants are then found and used to perform the interpolation for general point along these directions.[33] This improves the interpolated dispersion in the low-frequency region.

Along the Σ direction, the phonons at a wave vector between Γ and X are classified as $7\Sigma_1+3\Sigma_2+5\Sigma_3+6\Sigma_4$. Two transverse-acoustic (TA) branches, TA(Σ_3) and TA(Σ_4), are found to have imaginary frequencies. As the phonon wave vector varies from Γ to X, both TA(Σ_3) and TA(Σ_4) are initially stable, then the TA(Σ_3) mode becomes unstable, followed by the TA(Σ_4) mode. The tilt mode at the X point is on the Σ_4 branch and has the largest magnitude imaginary frequency in the whole Brillouin zone, which is consistent with the observed tetragonal-orthorhombic structural phase transition.

Fil *et al.*[34] proposed a renormalization of the phonon spectrum due to a Jahn-Teller electron-phonon interaction. In their model, interband transitions from the $d_{x^2-y^2}$ to the $d_{3z^2-r^2}$ Cu orbitals cause the renormalization, resulting in significant frequency reduction for the highest-lying Σ_3 branches. In particular they found a dramatic softening of frequencies of the highest Σ_3 modes around X, which have quadrupolar character, in qualitative agreement with experiment. Previously, LDA calculations of this dispersion have not been available for comparison. The present calculations show a phonon frequency change of about 5.7 THz (190 cm^{-1}) from Γ to X in the highest Σ_3 branch. This is in good agreement with the change of 5.1 THz observed in neutron-scattering experiment.[23] The frequency change in the model calculation of Fil *et al.* is about 11 THz. The present result lends support to the pair potential model studies by Chaplot *et al.*,[23] which showed that the effect investigated by Fil *et al.*[34] plays at most a very minor role.

Along the Δ direction, phonons are represented as $7\Delta_1+2\Delta_2+5\Delta_3+7\Delta_4$. While the highest frequency Δ_3 branch shows little dispersion, the highest Δ_1 branch exhibits a strong dip between the Γ and Z points, with a minimum near the boundary of the first Brillouin zone. This behavior of the calculated dispersion is in excellent agreement with the experimental phonon dispersions of $La_{1.9}Sr_{0.1}CuO_4$,[23] while a simple free-carrier treatment (neglecting band-structure effects) is inadequate.[23]

As may be expected from the strong two-dimensional characteristics of the electronic structure, most calculated optic phonon bands exhibit little dispersion along the $(0,0,\xi)$ direction (not shown). One exception is a phonon branch starting from an A_{1g} mode (198 cm^{-1}) at Γ and ending at an A_{2u} mode (360 cm^{-1}) at Z, which exhibits a change of 162 cm^{-1}, generally in agreement with the measured phonon dispersion in $La_{1.9}Sr_{0.1}CuO_4$ along the $(0,0,\xi)$ direction. However, the experimental branch showing the largest dispersion was assigned as starting from an A_{2u} mode at Γ,[22] which is not supported by our calculation.

IV. CONCLUSION

We have performed first-principles linear response calculations for the tetragonal structure of La_2CuO_4 and have obtained phonon frequencies and eigenvectors in the full Brillouin zone. Generally good agreement is obtained with experiment. Underestimates of the lowest-lying branches, which involve motion of the apical oxygen atoms parallel to the CuO_2 planes, are attributed to anharmonic stiffening of these frequencies in the low-temperature orthorhombic phase. The good agreement with experiment of the highest frequency Σ_3 branch indicates that phonon renormalization, due to a Jahn-Teller electron-phonon interaction, is unlikely.

ACKNOWLEDGMENTS

We are pleased to acknowledge useful discussions with M. Wensell, C. LaSota, X. Wan, and U. Waghmare. This work was supported by National Science Foundation Grant No. DMR-9404954. Computations were carried out at the Cornell Theory Center.

[1] I. Pintschovius and W. Reichardt, in *Physical Properties of High Temperature Superconductors IV*, edited by D. M. Ginsburg (World Scientific, Singapore, 1994), p. 295.

[2] J. P. Franck, in *Physical Properties of High Temperature Superconductors IV*, edited by D. M. Ginsburg (World Scientific, Singapore, 1994), p. 189.

[3] A. P. Litvinchuk, C. Thomsen, and M. Cardona, in *Physical Properties of High Temperature Superconductors IV*, edited by D. M. Ginsburg (World Scientific, Singapore, 1994), p. 375.

[4] See B. Brandow, Phys. Rep. **296**, 1 (1998) for a recent review.

[5] P. Bŏni, J. D. Axe, G. Shirane, R. J. Birgeneau, D. R. Gabbe, H. P. Jenssen, M. A. Kastner, C. J. Peters, P. J. Picone, and T. R. Thurston, Phys. Rev. B **38**, 185 (1988).

[6] R. Cohen, W. Pickett, and H. Krakauer, Phys. Rev. Lett. **62**, 831 (1989).

[7] H. Krakauer, W. E. Pickett, and R. E. Cohen, Phys. Rev. B **47**, 1002 (1993).

[8] D. J. Singh, Solid State Commun. **98**, 575 (1996).

[9] R. E. Cohen, W. E. Pickett, and H. Krakauer, Phys. Rev. Lett. **64**, 2575 (1990).

[10] C. O. Rodriguez, A. I. Liechtenstein, I. I. Mazin, O. Jepsen, O. K. Anderson, and M. Methfessel, Phys. Rev. B **42**, 2696 (1990).

[11] R. Kouba and C. Ambrosch-Draxl, Phys. Rev. B **56**, 14 766 (1997).

[12] R. Yu and H. Krakauer, Phys. Rev. B **49**, 4467 (1994); Phys. Rev. Lett. **74**, 4067 (1995); C.-Z. Wang, R. Yu, and H. Krakauer, *ibid.* **72**, 368 (1994).

[13] R. M. Sternheimer, Phys. Rev. **96**, 951 (1954); G. D. Mahan, Phys. Rev. A **22**, 1780 (1980); S. Baroni, P. Giannozi, and A. Testa, Phys. Rev. Lett. **58**, 1861 (1987).

[14] G. P. Kerker, J. Phys. C **13**, L189 (1980).

[15] E. Wigner, Phys. Rev. **46**, 1002 (1934).

[16] H. J. Monkhorst and J. D. Pack, Phys. Rev. B **13**, 5188 (1976).

[17] M. Methfessel and A. T. Paxton, Phys. Rev. B **40**, 3616 (1989).

[18] S. de Gironcoli, Phys. Rev. B **51**, R6773 (1995).

[19] L. F. Mattheiss, Phys. Rev. Lett. **58**, 1028 (1987); J. M. Longo

and P. M. Raccah, J. Solid State Chem. **6**, 526 (1973).
[20] R. T. Collins, Z. Schlesinger, G. V. Chandrashekhar, and M. W. Shaffer, Phys. Rev. B **39**, 2251 (1989).
[21] R. Henn, A. Wittlin, M. Cardona, and S. Uchida, Phys. Rev. B **56**, 6295 (1997); R. Henn, J. Kircher, and M. Cardona, Physica C **269**, 99 (1996).
[22] L. Pintschovius, N. Pyka, W. Reichardt, A. Yu. Rumiantsev, N. L. Mitrofanov, A. S. Ivanov, G. Collin, and P. Bourges, Physica C **185-189**, 156 (1991).
[23] S. L. Chaplot, W. Reichard, L. Pintschovius, and N. Pyka, Phys. Rev. B **52**, 7230 (1995).
[24] G. Burns and F. H. Dacol, Phys. Rev. B **41**, 4747 (1990).
[25] The elements of the dynamical matrix at Γ should satisfy the acoustic sum rule, which requires $\Sigma_{j,\beta} D_{i,\alpha,j,\beta}(\mathbf{q}=0)=0$. In actual calculations, however, this rule is slightly violated. This is because the exchange-correlation term in the total energy of a crystal is computed on a finite grid of points, instead of an integration in real space over the unit cell. This approximation breaks the invariance of the total energy with respect to arbitrary homogeneous translations, and leads to small violations. Since the violation is small, we have enforced the acoustic sum rule by making a compensation on the largest dynamical matrix element of the relevant column. With such a treatment, the phonon frequencies of acoustic modes at Γ become exactly zero from the original magnitude of about 25 cm^{-1}. This correction has a negligible effect on the higher frequency modes and relatively larger effects on the low frequency modes.
[26] R. E. Cohen, W. E. Pickett, H. Krakauer, and L. L. Boyer, Physica B **150**, 61 (1988).
[27] W. E. Pickett, R. E. Cohen, and H. Krakauer, Phys. Rev. Lett. **67**, 228 (1991).
[28] R. E. Cohen, W. E. Pickett, L. L. Boyer, and H. Krakauer, Phys. Rev. Lett. **60**, 817 (1988).
[29] R. E. Cohen, W. E. Pickett, H. Krakauer, and D. A. Papaconstantopoulos, Phase Transit. **22**, 167 (1990).
[30] C. LaSota, C.-Z. Wang, R. Yu, and H. Krakauer, Ferroelectrics **194**, 109 (1997); (unpublished).
[31] W. Zhong and D. Vanderbilt, Phys. Rev. Lett. **74**, 2587 (1995).
[32] W. Weber, Phys. Rev. Lett. **58**, 1371 (1987).
[33] C.-Z. Wang, R. Yu, and H. Krakauer, Phys. Rev. B **53**, 5430 (1996).
[34] D. V. Fil, O. I. Tokar, A. L. Shelankov, and W. Weber, Phys. Rev. B **45**, 5633 (1992).